

The Study of Structure and Transitional Phases in $\text{Ba}_{0.95}\text{Bi}_{0.05}\text{Ti}_{1-x}\text{Fe}_x\text{O}_3$ Ceramics Synthesized by Solid State Route

Gouitaa Najwa^{1,*}, Lamcharfi Taj-dine^{1,*}, Bouayad Lamfaddal¹, Abdi Farid¹, Ounacer Mohamed² and Sajieddine Mohammed²

* najwa.gouitaa@gmail.com, lamcharfi_taj@yahoo.fr

¹ Signals, Systems and Components Laboratory (LSSC), Electrical Engineering Department, University Sidi Mohamed Ben Abdellah USMBA, Morocco

² Physic of Materials Laboratory, FST, University Sultan Moulay Slimane, Beni-Mellal, Morocco

Received: November 2020

Revised: January 2021

Accepted: February 2021

DOI: 10.22068/ijmse.2058

Abstract: The structural and dielectric properties of iron and bismuth co-substituted BaTiO_3 ceramic with the formula: $\text{Ba}_{0.95}\text{Bi}_{0.05}\text{Ti}_{1-x}\text{Fe}_x\text{O}_3$ for $x=0.00$ to 1.00 , synthesized by solid state route, were characterized. The X-ray diffraction results showed a tetragonal phase for $x=0.00$. While for $x=0.40$ to 0.80 we observed a coexistence of tetragonal, hexagonal and pseudo-cubic phases. At $x=1.00$ only the pseudo-cubic phase is present and the other phase disappeared. The Raman results indicated the existence of tetragonal band for $x \leq 0.40$, and an appearance of characteristic bands of Fe^{3+} ions for Fe content of higher than 0.4 . The SEM micrographs showed an increase in grain size with the increase of Fe content and it reached a maximum at $x=0.40$. The Mossbauer spectroscopy indicated that the samples are paramagnetic at room temperature and that the Fe is oxidized under Fe^{3+} with no existence of Fe^{2+} or Fe^{4+} ions. The temperature dependence of dielectric permittivity was investigated in the frequency range from 20 Hz to 2 MHz. The results showed three dielectric relaxation phase transitions from a rhombohedral ferroelectric to orthorhombic ferroelectric (T_{R-O}) then to a tetragonal ferroelectric phase (at T_{O-T}), and finally to cubic paraelectric at the Curie temperature (T_C). In addition, the temperature of phase transition shifted to the lower temperature with the increase of Fe content for all the phase transitions. And the maximum of dielectric permittivity increased for T_{R-O} while for T_{T-O} and T_m phases transitions, it reached a maximum at $x=0.60$ and $x=0.80$ respectively and then decreased.

Keywords: Structural, dielectric, BaTiO_3 , solid state, SEM, Mossbauer, paramagnetic, phase transition, Curie temperature.

1. INTRODUCTION

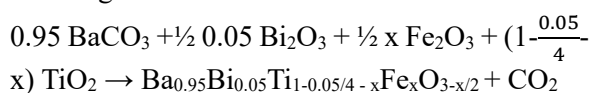
Multiferroic crystalline compounds are currently the subject of extensive research, due to their potential applications in the emerging field of spintronics, information storage and multi-state memory storage devices [1, 2, 3]. In order to explore the possibility of synthesizing a materials with superior multiferroic performances, different approaches are underway and the most used approach is to substitute magnetic ions such as transition metal ions (Fe^{3+} , Co^{2+} , Ni^{2+} , Mn^{2+} , etc.) in ferroelectric materials [4, 5]. In the ferroelectric family, the barium titanate (BaTiO_3) is the most widely used ferroelectric material and, even after seventy-five years of its discovery, it remained an essential material with excellent dielectric [6, 7], optical [8], piezoelectric [9] and ferroelectric [10] properties. The BaTiO_3 ceramic can exist in different polymorphs at different temperatures: hexagonal $P_{63/mmc}$ (at $T > 1460^\circ\text{C}$), cubic P_{m3m} (at $130^\circ\text{C} < T < 1460^\circ\text{C}$), P_{4mm}

tetragonal (at $0^\circ\text{C} < T < 130^\circ\text{C}$), orthorhombic A_{mm2} (at $-90^\circ\text{C} < T < 5^\circ\text{C}$) and the rhombohedral crystal structure $R3m$ (at $T < -90^\circ\text{C}$) [11, 12]. Alternatively, doping with various transition metal ions such as Fe, Co, Ni, Mn on Ti sites can also lead to the formation of hexagonal polymorphs at room temperature [13, 14]. Recently, the effect of Fe doping BaTiO_3 ceramic on the structural evolution from the tetragonal perovskite phase to the hexagonal phase, prepared by the solid route, has been studied [15, 16]. It is confirmed by several studies that doping with Fe promotes the formation of the hexagonal phase [17]. Although the Fe substitution BaTiO_3 ceramic (BTF) decreases the dielectric properties of the latter by reduction of the dielectric constant and displacement of the temperature of the phase transition to the higher temperatures [4, 18]. It has been also reported that the Bi substituted BaTiO_3 ceramic into the Ba site achieve a maximum dielectric constant at $x=0.05$ [19]. And the structure of these ceramics was reported to be

tetragonal for contents inferior to 0.10 of Bi [19, 20]. In the previous work we have studied the structural and dielectric evolution of Fe doped BaTiO₃ ceramic [17]. And in the other work we have studied the effect of Bi and Fe co-substitution on structural and dielectric properties of BaTiO₃ up to 0.20 of Fe content and the concentration of Bi fixed at 0.0521. In this work we have synthesis the Ba_{0.95}Bi_{0.05}Ti_{1-x}Fe_xO₃ ceramics for x=0.00 to 1.00 and studied the influence of Bi co-substitution on the structural and dielectric properties of BTF ceramics.

2. EXPERIMENTAL PROCEDURES

The Ba_{0.95}Bi_{0.05}Ti_{1-x}Fe_xO₃ ceramics for x=0.00 to 1.00 were prepared by the conventional solid-state method using the high-purity oxides BaCO₃, Bi₂O₃, TiO₂ and Fe₂O₃. The doping site of Fe and Bi ions in BaTiO₃ was controlled by stoichiometric proportions of raw materials allowing to the reaction:



The starting powders were weighted in stoichiometric proportion and milled under acetone for 4h. After that the powders were dried at 80°C for 24h. The dried powders were mixed using agate mortar for 30 min and then de-carbonated and pre-reacted by calcining in alumina at 1100°C for 4h. After calcination, the powders were mixed for 30 min. The crystal structure, phase purity, space groups, and lattice parameters of the product (Ba_{0.95}Bi_{0.05}Ti_{1-x}Fe_xO₃) were characterized by X-ray diffraction (XPRT-PRO with Cu K α radiation with $\lambda=1.5406\text{\AA}$) and Raman spectrum was recorded at room temperature. The valence of Fe was analyzed with the ⁵⁷Fe Mössbauer spectra at room and all the values of isomer shift within this paper are related to the α -Fe standard.

The calcined powders were pressed into pellets, after adding few drops of 1 wt % Polyvinyl Alcohol (PVA) as a binder, and sintered in air at 1200°C for 6h. The investigations of the microstructure of the pellets were performed using by a scanning electron microscope (SEM). And the dielectric properties as function of frequency and temperature were studied with Agilent E4980A (20 Hz-2 MHz).

3. RESULTS AND DISCUSSION

3.1. X-RAY DIFFRACTION RESULTS

The X-ray diffraction results of Ba_{0.95}Bi_{0.05}Ti_{1-x}Fe_xO₃ powders for x=0.00 to 1.00 calcined at 1100°C for 4h is shown in Figure.1. The spectrum of Ba_{0.95}Bi_{0.05}TiO₃ (x=0.00) shows the existence of peaks characteristic of the quadratic (tetragonal) phase [21] without the presence of other secondary phases. For x=0.20, the results were discussed in our previous work [22] and show the appearance of hexagonal phase with coexistence of tetragonal phase. While for x=0.40 to 0.80 we can observe the presence of multiphases indexed to tetragonal, hexagonal and pseudo-cubic phase. And for x=1.00 only the pseudo-cubic phase is observed.

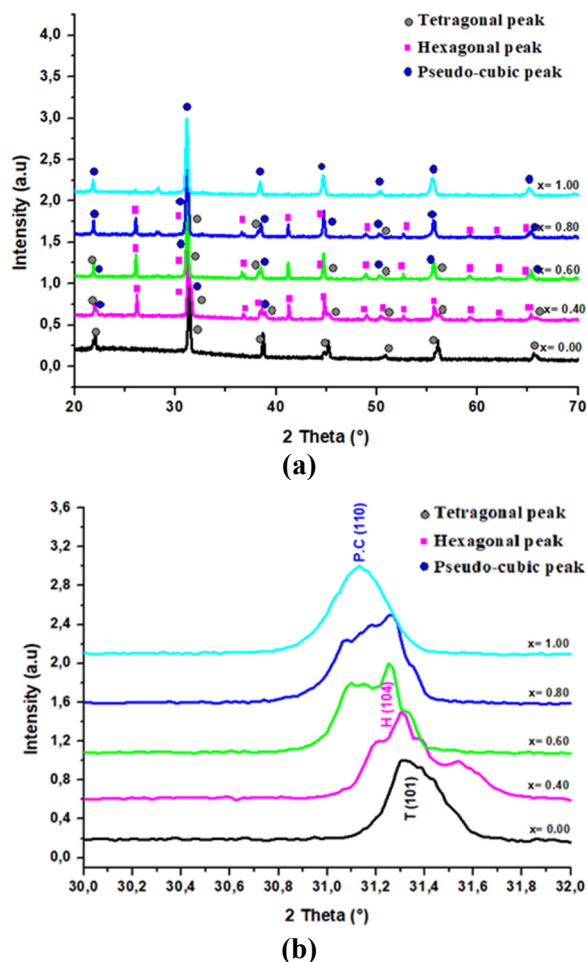


Fig. 1. a) X-ray diffractogram of Ba_{0.95}Bi_{0.05}Ti_{1-x}Fe_xO₃ ceramics for x=0.00 to 1.00. **b).** Zoom on T(101), H(104) et P-C (110) peaks characteristic of tetragonal, hexagonal and pseudo cubic phase respectively.

As it is shown in Figure. 1.b, the tetragonal peaks are present for the $\text{Ba}_{0.95}\text{Bi}_{0.05}\text{Ti}_{1-x}\text{Fe}_x\text{O}_3$ substituted at $x=0.00$. At $x=0.40$ the tetragonal peak is still present with shifting of this peak towards the high angles which confirms the incorporation of iron in the $\text{Ba}_{0.95}\text{Bi}_{0.05}\text{Ti}_{1-x}\text{Fe}_x\text{O}_3$ ceramic (BBTO). And a new peaks appear which are characteristics of the hexagonal and pseudo cubic phases, which indicates the coexistence of tree phases tetragonal, hexagonal and pseudo cubic. For $x=0.60$ and 0.80 we first notice an increase in the intensity of the peak characteristics of the hexagonal and pseudo-cubic phases and a decrease of these characteristics of the tetragonal phase. Whereas for $x=1.00$ the structure is completely transformed to a pure pseudo-cubic structure without the presence of other phases. From these results, it can be concluded that Bi co-substitution delays the appearance of the hexagonal phase induced by the Fe substitution and maintains the coexistence of tree phases in a large domain of Fe-substitution. According to our knowledge these results are not found in previous works.

3.2. RAMAN RESULTS

We have studied the structural properties of $\text{Ba}_{0.95}\text{Bi}_{0.05}\text{Ti}_{1-x}\text{Fe}_x\text{O}_3$ ceramics ($x=0.00$ to 1.00) by Raman spectroscopy (Figure. 2). We can distinguish two concentration ranges: the first for rates below 0.40 (Figure. 2.a) and the second beyond 0.40 (Figure. 2.b).

The Raman spectrum of $\text{Ba}_{0.95}\text{Bi}_{0.05}\text{Ti}_{1-x}\text{Fe}_x\text{O}_3$ powders for $x=0.00, 0.20$ and 0.40 (Figure. 2.a) is indexed in quadratic symmetry [18, 23]. These spectra are the same of that of pure BaTiO_3 with the appearance of the A_{1g} mode around 716 cm^{-1} . The $A_1(\text{TO}_1)$ mode is detected around 177 cm^{-1} in the vibrational spectrum of the BBTO corresponding to the Ti atoms vibrations. And the mode at 305 cm^{-1} , assigned to the $B_1/E(\text{TO}_2)$ mode, characteristic of quadratic symmetry, is observed in the case of BBTO ($x=0.00$) and it corresponds to the asymmetric vibrations Ti-O. The intensity of this peak decreases with increasing Fe levels which confirms that the rate of the quadratic phase of these powders decreases with increasing Fe levels from 0.00 to 0.40 . The $A_1(\text{TO}_2)$ mode describing the symmetrical O-Ti-O vibrations, is characterized by a resonance which also varies with the strong

substitution of Fe at B site of the perovskite structure. The last mode $A_1(\text{LO}_2)/E(\text{LO}_3)$ at 669 cm^{-1} , reflects a large concentration of polar octahedra $[\text{TiO}_6]$ undergoing a quadratic distortion.



Fig. 2. Raman spectra of $\text{Ba}_{0.95}\text{Bi}_{0.05}\text{Ti}_{1-x}\text{Fe}_x\text{O}_3$ ceramics for **a)** $x = 0.00$ to 0.40 , and **b)** $x = 0.60$ to 1.00 .

The A_{1g} mode (octahedral breathing mode) observed around 716 cm^{-1} is chemical in nature and is not related to the structural distortions of the crystal lattice. This mode is inactive in Raman for simple perovskites since it is symmetrical and does not cause a change in polarizability. However, this mode becomes active in Raman for complex perovskites having two different cations at the center of the BO_6 octahedron (for example $\text{Fe}^{3+}/\text{Ti}^{4+}$) or even when the site ion A (Ba^{2+} in this case) is replaced by a donor dopant Bi^{3+} [24, 25]. The appearance of the A_{1g} mode confirms the fact that Fe substituted Ti on B site.

From $x=0.60$ (Figure. 2.b), the spectra undergo a

significant changes. However, we observe the existence of A_{1g} , E_{1g} and E_{2g} peaks which are attributed to Fe^{3+} ions (indexed in red). This confirms that the chemical environment at B sites has indeed been modified between $x=0.60$ and $x=1.00$. This is related probably to the presence of Fe^{3+} at B sites which increases as a function of x relative to the Ba^{2+}/Bi^{3+} cations. It should be noted that the peaks $A_1(TO_2)$ and $B_1/E(TO_2)$ characteristics of the tetragonal phase are always present for the levels of Fe more than 0.60.

3.3. SEM RESULTS

The morphologies of the $Ba_{0.95}Bi_{0.05}Ti_{1-x}Fe_xO_3$ pellets for $x=0.00$ to 1.00, sintered at $1200^\circ C$ for 6h, were observed by SEM and are shown in Figure. 3. The micrographs indicate that the grains have a relatively homogeneous shape and a porosity which differs from one sample to another. Figures. 3.c, d and e ($x=0.40$, 0.60 and 0.80) indicate that the particles have a hexagonal shape. In fact, with the increase of the Fe substitution, the shape of the grain is no longer spherical as at $x=0.00$.

The evolution of the average grain size as function of Fe contents is shown in Figure. 4. The graph shows a small decrease in the average grain size from 0.00 to 0.20 of the Fe levels, then it increases rapidly at $x=0.40$. However, when the Fe concentration is 0.40, there is coexistence of small and large grains in SEM micrographs. It indicates that addition of Fe leads to abnormal grain growth in this sample. After this concentration the grain size decreases to $x=0.60$. And beyond it increases slightly. Therefore, from these results it can be concluded that the evolution of the grain size is not linear, due probably to the instability of the phase structure as a function of the Fe rate which is observed in XRD results.

3.4. MOSSBAUER SPECTROSCOPY

The experiments graphs of Mössbauer spectroscopy of ^{57}Fe of $Ba_{0.95}Bi_{0.05}Ti_{1-x}Fe_xO_3$ is shown in Figure.5. Despite a relatively long counting time (ten days), no trace of magnetic component was detected in the spectra performed for $Ba_{0.95}Bi_{0.05}Ti_{1-x}Fe_xO_3$

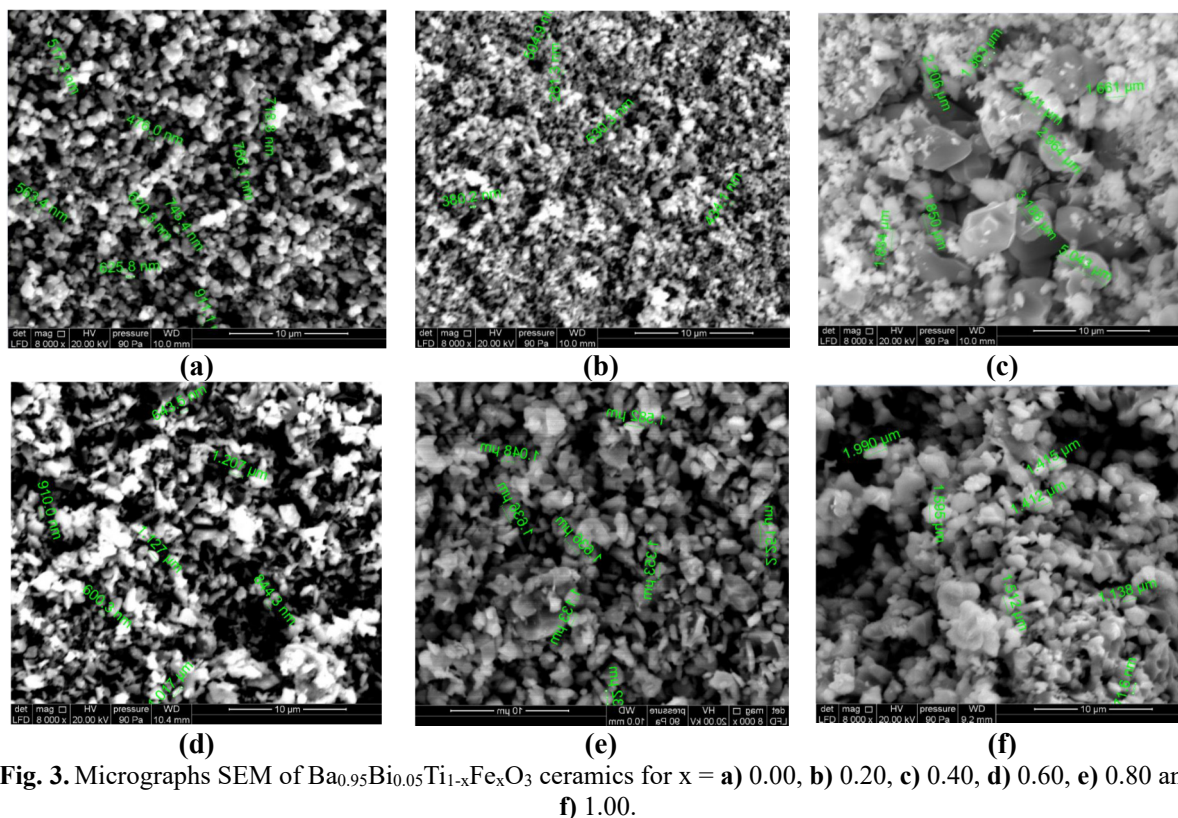


Fig. 3. Micrographs SEM of $Ba_{0.95}Bi_{0.05}Ti_{1-x}Fe_xO_3$ ceramics for $x =$ a) 0.00, b) 0.20, c) 0.40, d) 0.60, e) 0.80 and f) 1.00.

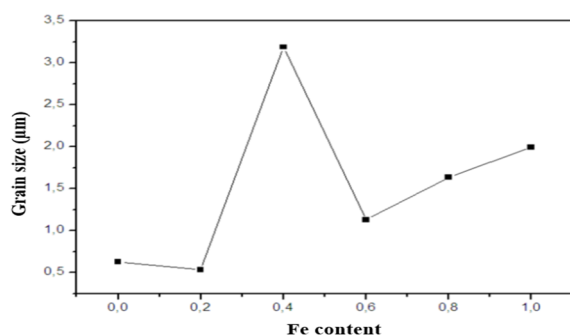


Fig. 4. Grain size evolution of $\text{Ba}_{0.95}\text{Bi}_{0.05}\text{Ti}_{1-x}\text{Fe}_x\text{O}_3$ ceramics as function of Fe content.

ceramics ($x = 0.20, 0.40, 0.60, 0.80$ and 1.00), which shows that our ceramics are in paramagnetic state. Consequently, no trace of divalent iron is observed within the detection limit of the technique.

The values of $\text{IS}=0.24$ mm/s and $\text{QS}=0.40$ mm/s (shown in Table. 1) are typical of Fe^{3+} ions in an octahedral environment [26, 27, 28]. Therefore, we can deduce that in the phase $\text{Ba}_{0.95}\text{Bi}_{0.05}\text{Ti}_{1-x}\text{Fe}_x\text{O}_3$, there are two iron sites, both occupied by Fe^{3+} and surrounded by a deformed octahedron of oxygen atoms with different degrees of

distortion.

All the spectra in Figure. 4 lead to the same results: an asymmetry of the lines of the quadrupole doublet D_1 is systematically observed for these ceramics ($\text{QS}=0.40$). Whereas for the D_2 doublet, the parameter of the quadrupole separation QS decreases largely with the substitution in Fe at $x=0.80$ which shows that D_2 doublet presents a quadratic symmetry which becomes stable at this doping rate.

3.5. DIELECTRIC PROPERTIES

The Figure. 6 shows the evolution of the dielectric permittivity, as a function of temperature from the room temperature to 600°C and at different frequencies (from 5 KHz to 2 MHz), for $\text{Ba}_{0.95}\text{Bi}_{0.05}\text{Ti}_{1-x}\text{Fe}_x\text{O}_3$ samples ($x=0.00, 0.20, 0.40, 0.60, 0.80$ and 1.00). The spectra show three dielectric anomalies at different temperatures. Based on the literature [29, 30] we can distinguish three phase transitions. The first maximum at low temperature $\sim 150^\circ\text{C}$, corresponds to a phase transition from the ferroelectric rhombohedral phase to the ferroelectric orthorhombic phase $\text{T}_{\text{R-O}}$. This anomaly persists for all ceramics but at

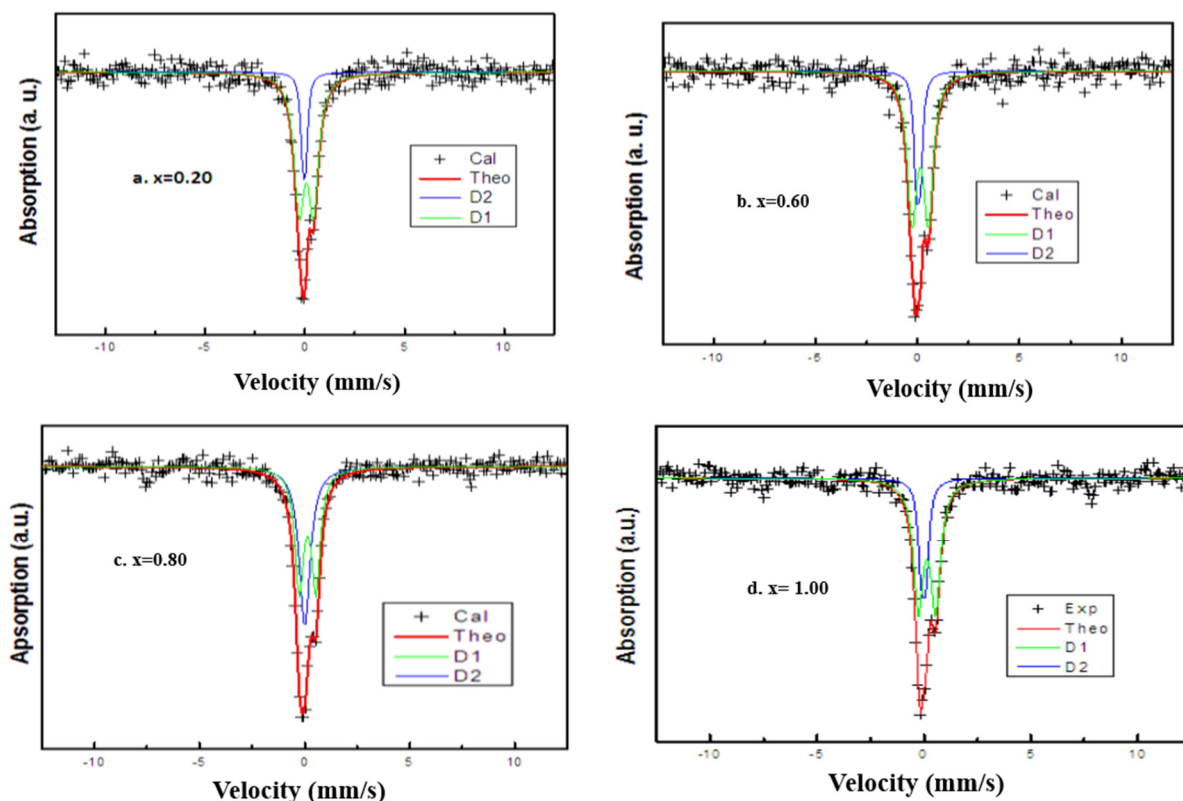


Fig. 5. Mössbauer spectra of $\text{Ba}_{0.95}\text{Bi}_{0.05}\text{Ti}_{1-x}\text{Fe}_x\text{O}_3$ ceramics for $x=$ a) 0.20, b) 0.60, c) 0.80 and d) 1.00.

Table 1. The hyperfine parameters of Ba_{0.95}Bi_{0.05}Ti_{1-x}Fe_xO₃ ceramics (x = 0.20, 0.40, 0.60, 0.80 and 1.00).

x	Doublets	Area	IS (mm.s ⁻¹)	QS (mm.s ⁻¹)	FWHM
0.20	Doublet-1	74.80	0.24	0.4	0.28
	Doublet-2	25.20	0.14	0.10	0.13
0.60	Doublet-1	74.80	0.24	0.4	0.28
	Doublet-2	25.20	0.14	0.10	0.13
0.80	Doublet-1	54.40	0.24	0.40	0.25
	Doublet-2	45.60	0.10	0.001	0.31
1.00	Doublet-1	70.90	0.24	0.40	0.28
	Doublet-2	29.10	0.09	0.11	0.17



Fig. 6. Temperature dependence of dielectric permittivity of Ba_{0.95}Bi_{0.05}Ti_{1-x}Fe_xO₃ ceramics for x=0.00 to 1.00.



different temperatures. The second maximum at intermediate temperatures ($\sim 500^\circ\text{C}$) corresponds to a phase transition from the ferroelectric orthorhombic phase to the ferroelectric tetragonal phase T_{O-T} . While the third maximum at high temperatures ($\sim 600^\circ\text{C}$) corresponds to a phase transition from the tetragonal ferroelectric phase to the cubic paraelectric phase T_m .

These three phase transitions show a dielectric relaxation phenomenon in all these ceramics which is very clear at $x=0.40$, with a maximum of dielectric permittivity which shifts towards high temperatures with increasing frequency. We also note that the three maximums of phase transitions are diffuse and present a strong diffuse character with increasing frequency.

According to the curves of the evolution of T_{R-O} , T_{O-T} and T_m as a function of the Fe content (Figure. 7), we can notice that the two phases temperature T_{O-T} and T_m move towards the low temperatures with the increase in the Fe level. This decrease in T_m is also observed for BaTiO_3 ceramics doped with Fe that we have reported before [17] and it is attributed to the phenomenon of coexistence of different phases [30].

In general, cations with a smaller ionic radius tend to produce stronger covalent bonds with oxygen ligands. The replacement of the Fe^{3+} ion ($r_i=0.64\text{\AA}$) by a high ferroelectric Ti^{4+} ion forms polar clusters of BaTiO_3 which lead to decentering the Ti^{4+} cations ($r_i=0.605\text{\AA}$) within the octahedral cage, by hybridization between the Ti 3d orbit and the O 2p orbitals. This forms a long-range Coulomb field and leads directly to a decrease in the transition temperature [31]. While for the T_{R-O} phase transition there is a displacement of the latter towards the high temperatures for x less than 0.40 then towards the low temperatures beyond this Fe content.

In addition we note that the maximum of the dielectric permittivity ($\epsilon_{r,\max}$) of the first phase transition T_{R-O} increases with the increase of the Fe content while the other two maximums of the dielectric permittivity reach a maximum for $x=0.60$ (for T_m) and $x=0.80$ (for T_{O-T}) then decrease. It is well established that the high value of the dielectric permittivity of the composition is due to the presence of three phases in these ceramics at $x=0.60$ and 0.80 , detected by X-ray diffraction. In addition, the ionic radius of Ba^{2+} ($r_i=1.35\text{\AA}$) larger than that of Bi^{3+} ($r_i=1.2\text{\AA}$) and the heavier atomic number of bismut ($z=83$) that

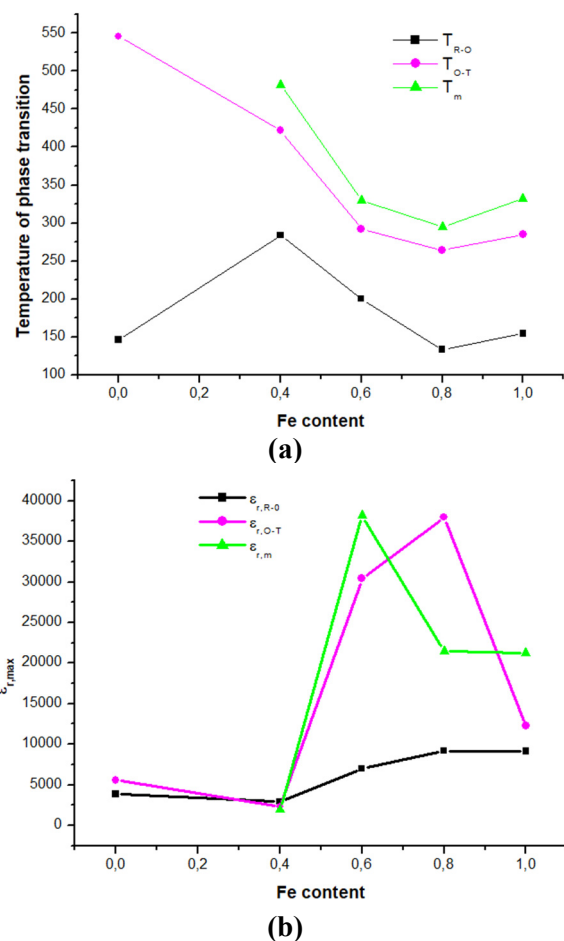


Fig. 7. Evolution of a) temperature of phase transition and b) dielectric permittivity of the three phase transition T_{R-O} , T_{O-T} and T_m .

barium ($z=56$) suggest that the dipole moment associated with the spontaneous polarization of the Ba^{2+} ions is greater than the dipole moment associated with the Bi^{3+} ions due to the greater distance 'a' which separates the center of positive charge from negative charge center in the cation Ba^{2+} , as described by the relation $P=Qa$, where P is the dipole moment and Q is the quantity of charge [30]. For these reasons, the dielectric properties of BT co-substituted with Bi and Fe are improved compared to the BT material doped with Fe [17]. We can deduct from these results that the dielectric constant remains high values in a wide temperature range between T_{O-T} and T_m . By comparing the results obtained for $\text{Ba}_{0.95}\text{Bi}_{0.05}\text{TiO}_3$ ($x=0.00$) with those obtained by F. Bahri et al [32], we note that the value of $\epsilon_{r,\max}$ in our study is greater. This difference in value may be due to the formula used. However, these authors have created a

vacancy sites in A site using the following formula: $\text{Ba}_{1-x}\text{Bi}_{2x}/3\text{V}_x/3\text{TiO}_3$.

4. CONCLUSIONS

The $\text{Ba}_{0.95}\text{Bi}_{0.05}\text{Ti}_{1-x}\text{Fe}_x\text{O}_3$ ceramics were synthesized by the solid-state method. The XRD results confirm the existence of tetragonal phase for $x=0.00$. While for $x=0.40$ to 0.80 there is a coexistence of three phases which are tetragonal, hexagonal and pseudo-cubic. At $x=1.00$, the tetragonal and hexagonal phase disappear and only the pseudo-cubic phase persists. The SEM results show a homogenous grain shape in these ceramics and the grain size reaches a maximum at 0.40 of Fe content. The isomer shift in Mossbauer spectroscopy indicates the third oxidation state of iron. On the other hand, the evolution of dielectric properties as function of temperature shows the existence of three phase transitions T_{R-O} , T_{O-T} and T_m and the dielectric properties of Bi co-substituted BTF were improved compared with BTF ceramics.

5. CONFLICT OF INTEREST

The authors declare that they have no conflict of interest.

6. REFERENCES

- [1] Bibes, M and Barthélémy, A. "Towards a magnetoelectric memory" *Nat. Mater.*, 2008, 7, 425-426.
- [2] Lin, F and Shi, W. "Magnetic properties of transition-metal-codoped BaTiO_3 systems". *Journal of Alloys and Compounds*, 2009, 475, 64-69.
- [3] Catalan, G and Scott, J.F. "Physics and applications of bismuth ferrite". *Advanced Materials*, 2009, 21, 2463-2485.
- [4] Apostolova, I, Apostolov, A, Bahoosh, S.G, and Wesselinowa, J.M. "Origin of ferromagnetism in transition metal doped BaTiO_3 ", *Journal of Applied Physics*, 2013, 113 203904.
- [5] Kundu, T, Jana, A and Barik, P. "Doped barium titanate nanoparticles", *Bulletin of Materials Science*, 2008, 31, 501-505.
- [6] Li, W, Xu, Z, Chu, R, Fu, P, and Zang, G. "Structural and dielectric properties in the $(\text{Ba}_{1-x}\text{Ca}_x)(\text{Ti}_{0.95}\text{Zr}_{0.05})\text{O}_3$ ceramics", *Current Applied Physics*, 2012, 12, 748-751.
- [7] Pecharroman, C, Esteban-Betegon, F, Bartolome, J.F, Lopez-Esteban, S and Moya, J.S. "New Percolative BaTiO_3 -Ni Composites with a High and Frequency-Independent Dielectric Constant ($\epsilon_r \approx 80000$)", *Advanced Materials*, 2001, 13, 1541-1544.
- [8] Woldu, T, Raneesh, B, Sreekanth, P, Reddy, M.R, Philip, R and Kalarikkal, N. "Size dependent nonlinear optical absorption in BaTiO_3 nanoparticles", *Chemical Physics Letters*, 2015, 625, 58-63.
- [9] Wang, Z, Suryavanshi, A.P and Yu, M.-F. "Ferroelectric and piezoelectric behaviors of individual single crystalline BaTiO_3 nanowire under direct axial electric biasing", *Applied physics letters*, 2006, 89 -082903.
- [10] Bersuker, I. "On the origin of ferroelectricity in perovskite-type crystals". *Physics Letters*, 1966, 20, 589-590.
- [11] Al-Shakarchi E.K. "Dielectric properties of a BaTiO_3 ceramic prepared by using the freeze drying method". *Journal of the Korean Physical Society*, 2010, 57, 2, 245-250.
- [12] Kwei, G, Lawson, A, Billinge, S and Cheong, S. "Structures of the ferroelectric phases of barium titanate", *The Journal of Physical Chemistry*, 1993, 97, 2368-2377.
- [13] Samuvel, K and Ramachandran, K. "Structure, electrical and magnetic property investigations on Fe-doped hexagonal BaTiO_3 ", *Optik-International Journal for Light and Electron Optics*, 2016, 127, 1781-1786.
- [14] Osoro, G.M, Bregiroux, D, Thi, M.P and Levassort, F. "Structural and piezoelectric properties evolution induced by cobalt doping and cobalt/niobium co-doping in BaTiO_3 ", *Materials Letters*, 2016, 166, 259-262.
- [15] Qiu, S.Y, Li, W, Liu, Y, Liu, G.H, Wu, Y.Q, and Chen, N. "Phase evolution and room temperature ferroelectric and magnetic properties of Fe-doped BaTiO_3 ceramics", *Transactions of Nonferrous Metals Society of China*. 2010, 20(10), 1911-1915.

- [16] Dang, N. V, Thanh, T. D, Hong, L. V, Lam, V. D, and Phan, T.L. "Structural, optical and magnetic properties of polycrystalline $\text{BaTi}_{1-x}\text{Fe}_x\text{O}_3$ ceramics", Journal of Applied Physics, 2011, 110(4), 043914-043914-7.
- [17] Gouitaan, N, Lamcharfi, T, Bouayad, Mf, Abdi, F., Echadou, N.S and Hadi, N. "Dielectric anomalies of $\text{BaTi}_{1-x}\text{Fe}_x\text{O}_3$ ceramics for $x=0.0$ to 0.6 of Fe doping concentration", Asian Journal of Chemistry, 2017, 29, 10, 2143-2148.
- [18] Rani, A, Kolte, J, Vadla, S. S and Gopalan. P. "Structural, electrical, magnetic and magnetoelectric properties of Fe doped BaTiO_3 ceramics", Ceramics International, 2016, 42, 8010–8016.
- [19] Jiang, X.P, Zeng, M, Kowk, K.W and Chan, H.L.W. "Dielectric and Ferroelectric Properties of Bi-Doped BaTiO_3 Ceramics". Key Eng. Mater, 2007, 334, 977-980.
- [20] Vittayakorn, N. "Synthesis and dielectric properties of bismuth doped barium titanate (BaTiO_3) Ceramics", J. Appl. Sci. Res, 2006, 2 (12) 1319.
- [21] Gouitaa, N, Lamcharfi, T, Bouayad, L, Abdi, F, and Naciri Bennani, M. "Structural and dielectric properties of $\text{Ba}_{0.95}\text{Bi}_{0.05}\text{Ti}_{1-x}\text{Fe}_x\text{O}_3$ ceramics at $x=0.0$, 0.1 and 0.2 prepared by solid state method", Mediterranean Journal of Chemistry, 2019, 8(2), 220-227.
- [22] Yansen, W, Kim, D, Parwanta, K. J, Liu, C and Lee, B. W. "Rietveld analysis and multiferroic properties of Fe doped $\text{Ba}_{0.95}\text{Bi}_{0.05}\text{TiO}_3$ ceramics", Current Applied Physics, 2015, 15, 120-123.
- [23] Al-Naboulsi, T. 'Elaboration de poudres de titanates par mécanosynthèse et caractérisation électrique', Thèse de doctorat d'état à Toulouse 3, dans le cadre de École Doctorale Sciences de la Matière (Toulouse), soutenue le 12-04-2016.
- [24] Siny, I. G, Tao, R, Katiyar, R. S, Guo, R and Bhalla, A. S. "Cation Ordering Types and Dielectric Properties in the Complex Perovskite $\text{Ca}(\text{Ca}_{1/3}\text{Nb}_{2/3})\text{O}_3$ ", J. Phys. Chem. Solids, 1998, 59, 181.
- [25] Pokorny, J, Pasha, U. M, Ben, L, Thakur, O. P, Sinclair, D. C and Reaney, I. M. "Use of Raman spectroscopy to determine the site occupancy of dopants in BaTiO_3 ", J. Appl. Phys, 2011, 109, 114110.
- [26] Cotica, L.F, Zanatta, S.C, Rocha, M.A, Santos, I.A, Paesano, A. da Cunha, J.B.M and Hallouche, B. "Phase evolution and magnetic properties of a high-energy ball-milled hematite–alumina system", J. Appl. Phys, 2004, 94, 1307.
- [27] Dormani, J.L, Fiorani, D and Tronc, E., Adv. Chem. Phys, 1997, 98, 283.
- [28] Santos, I.A, Grande, H.L.C, Freitas, V.F, de Medeiros, S.N, Paesano Jr, A, Cotica and L.F, Radovanovic, E, J. Non-Cryst. Solids, 2006, 352, 3721.
- [29] Bourguiba, F, Dhahri, Ah, Tahri, T, Dhahri, J, Abdelmoula, N, Taibi, K and Hlil, E.K. "Structure properties and relaxor characteristics of the phases transformation in $\text{BaTi}_{0.5}(\text{Fe}_{0.33}\text{Mo}_{0.17})\text{O}_3$ perovskite ceramic", Journal of Alloys and Compounds, 2016, 675, 174-182.
- [30] Bourguiba, F, Dhahri, Ah, Tahri, T, Dhahri, J, Abdelmoula, N, Taibi, K and Hlil, E.K. "Effect of iron and tungsten substitution on the dielectric response and phase transformations of BaTiO_3 perovskite ceramic", Journal of Alloys and Compounds, 2016, 686, 675-683.
- [31] Kumar, A, Murari, N.M and Katiyar, R.S. "Investigation of dielectric and electrical behavior in $\text{Pb}(\text{Fe}_{0.66}\text{W}_{0.33})_{0.50}\text{Ti}_{0.50}\text{O}_3$ thin films by impedance spectroscopy", J. Alloys Compd, 2009, 469, 433-440.
- [32] Bahri, F, Simon, A, Khemakhem, H, and Ravez, J. "Classical or Relaxor Ferroelectric Behaviour of Ceramics with Composition $\text{Ba}_{1-x}\text{Bi}_{2x/3}\text{TiO}_3$ ", phys. stat. sol. (a), 2001, 184, No. 2, 459–464.